Electronic Depository Text

Figure S1 displays a backscatter electron (BSE) image of a typical well-crystallised vandenbrandeite fragment, with corresponding EDXA elemental maps of the same area, from sample BGS 756/1. The elemental maps reveal the presence and distribution of trace amounts of fine intercrystalline particles of magnesium silicate ($MgSiO_3$) and quartz (SiO_2) as minor contaminant minerals on the surfaces of the vandenbrandeite crystals. Al may be present in some fine particles, indicating that some particles may be magnesium-aluminium silicate ($(Mg,Al)SiO_3$). No other contaminant phases were detected by EDXA element mapping in sample BGS 756/1.

Vector images for all the simulated Raman modes are displayed in **Figures S2** to **S11** revealing the dominant vibration occurring in the structure at each frequency. It should be noted that very minor vibrations were observed occurring across the entire structure for each mode; this is attributed to the presence of small residual forces following the geometry optimisation performed on the system (all forces less than 1×10^{-3} eV Å^{-1}). A summary table listing all the simulated Raman peak positions and their modal assignment can be found in **Table 1** in the main paper along with comparisons to experimental measurements obtained in this study and those Raman spectra reported in the literature.

All eight images in **Figure S2** reveal multi-directional H-bonding vibrations between the OH^- ions which link the Cu-uranyl sheets. The simulated ν(OH···H) peak positions are at 3614, 3576, 3555, 3445, 3408, 3400, 3365 and 3229 cm^{-1}. **Figure S3** shows eight multi-directional vibrations of the free-hanging H atom bonded to an equatorial uranyl O atom, δ(UOH), occurring at 1044, 1018, 1009, 974, 969, 947, 943 and 917 cm^{-1}.

The first three vector images displayed in **Figure S4** (at 889, 878 and 850 cm^{-1}) are the uranyl axial asymmetric stretch, $\nu_3(UO_2)^{2+}_{axial}$, whereas the latter three images (at 828, 800 and 791 cm^{-1}) are assigned to the uranyl axial symmetric stretch $\nu_1(UO_2)^{2+}_{axial}$. Both these modes are known to be environmentally sensitive and are accompanied by δ(UOH) vibrations, probably due to the lightness of the H element compared to its nearest neighbours.

The first four vector images shown in **Figure S5** are attributed to more δ(UOH) vibrations at 780, 760, 734 and 624 cm^{-1}. **Figure S5e** and **f** are assigned to asymmetric and symmetric stretches of the U-O-Cu bonds, ν_3(U-O-Cu) and ν_1(U-O-Cu), in the vandenbrandeite sheets at 579 and 546 cm^{-1}, respectively. The final two vector images in **Figure S5** are asymmetric (at 496 cm^{-1}) and symmetric (493 cm^{-1}) O-Cu-O stretch, ν_3(O-Cu-O) and ν_1(O-Cu-O), modes, respectively. Some of the simulated Raman modes in **Figure S5** were also attributed to lower wavenumber positioned features shown in **Figure S6**. The ν_3(O-Cu-O) is, again, simulated at 464, 446 and 430 cm^{-1} (**Figure S6b-d**), the ν_1(O-Cu-O) mode at 403 and 382 cm^{-1} (**Figure S6e-f**) and another ν_3(U-O-Cu) peak at 372 cm^{-1} (**Figure S6g**). The first vector image in **Figure S6**, at 484 cm^{-1}, is attributed to asymmetric bending of the uranyl ion in the equatorial plane, $\nu_4(UO_2)^{2+}_{equatorial}$, whereas **Figure S6h** is assigned to another δ(UOH) vibration at 366 cm^{-1}. It should be noted that **Figures S5e-h** and **S6a-h** also display multi-directional movements in the free-hanging H atom (i.e., the δ(UOH) mode) due to the lightness of this element compared to its nearest neighbours.

Figure S7a and **e** displays the simulated vector image for the asymmetric stretching of the uranyl ion in the equatorial plane, $\nu_3(UO_2)^{2+}_{equatorial}$, positioned at 350 and 293 cm^{-1}, respectively. Six further δ(UOH) vibrations are revealed at 345, 320 and 309 cm^{-1} (**Figure S7b-d**) and 290, 277 and 268 cm^{-1} (**Figure S7f-h**). All five Raman vector images shown in **Figure S8** are assigned to the symmetric axial uranyl bending, $\nu_2(UO_2)^{21+}_{axial}$, mode with simulated peaks positioned of 246, 244, 239, 230 and 222 cm^{-1}. The remaining simulated vector images are assigned to general lattice vibrations in the vandenbrandeite crystal structure at 215, 203, 196, 187, 175 and 162 cm^{-1} (**Figure S9**) 156, 147, 132, 121, 114 and 109 cm^{-1} (**Figure S10**) and 99, 97, 78, 72, 57 and 43 cm^{-1} (**Figure S11**).

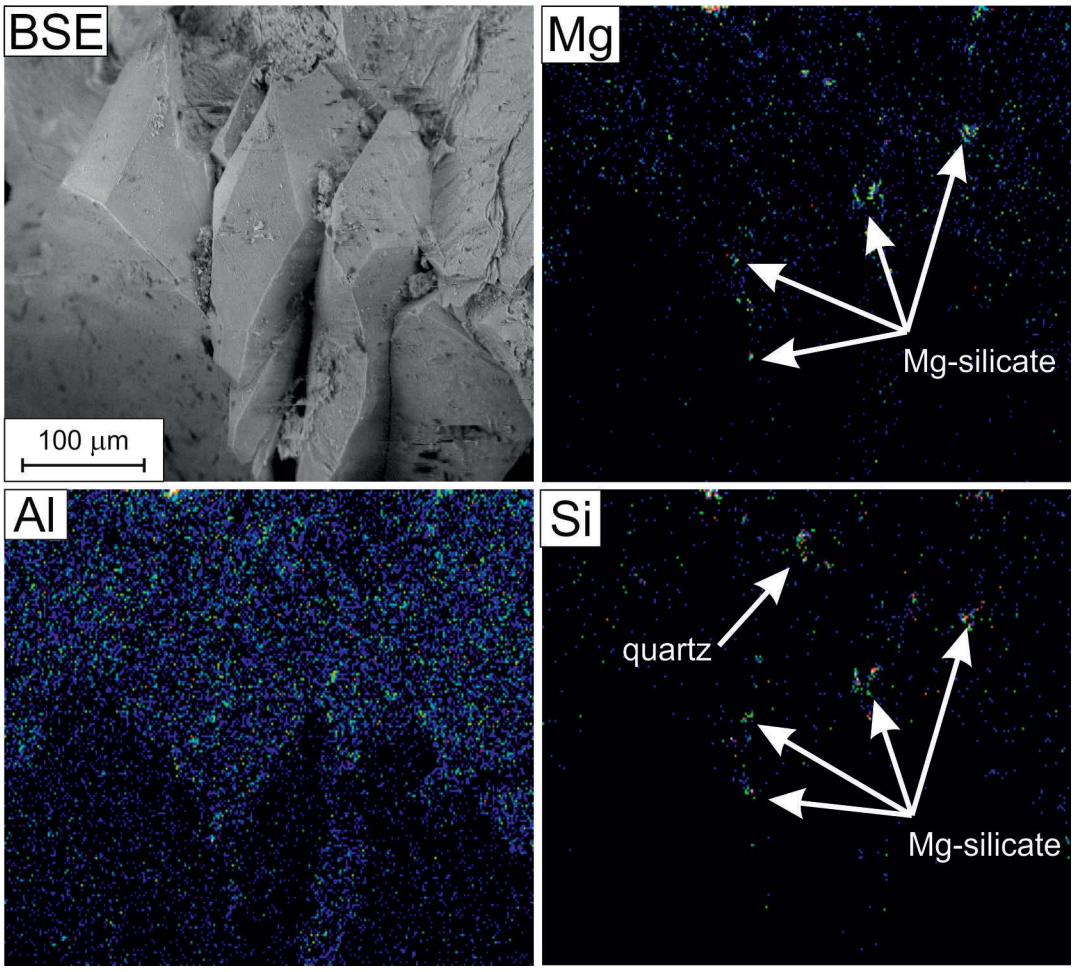

FIGURE S1: BSE image of a typical earthy vandenbrandeite fragment, with corresponding EDXA element maps of the same area, from sample BGS 756/1. The elemental maps reveal the presence and distribution of inclusions of copper sulphide (S), silica (Si), hydrotalcite (Mg-Al), and gypsum (Ca-S) as minor contaminant minerals within the vandenbrandeite groundmass.

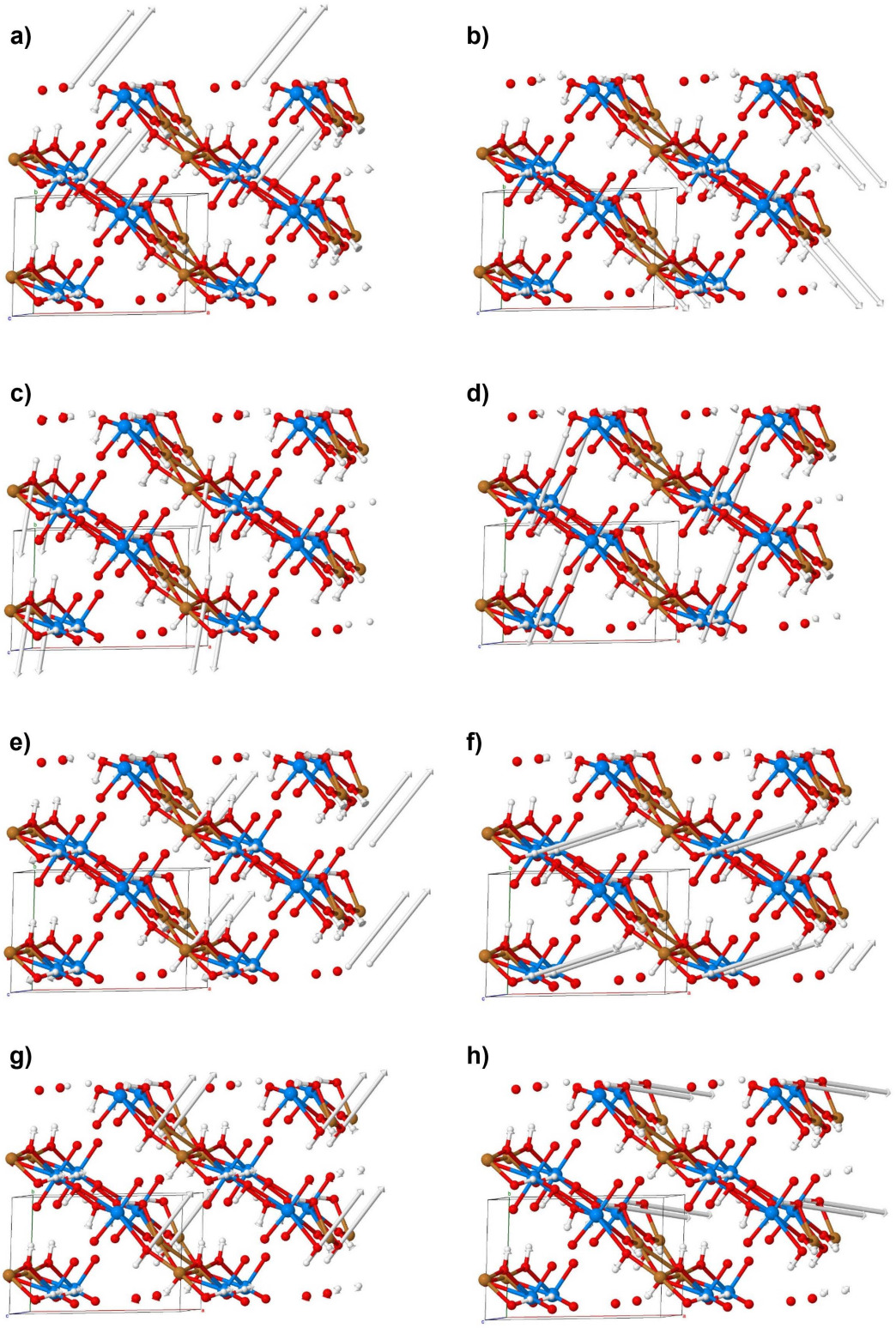

FIGURE S2: Raman vector H-bonding, *v*(OH···H), vibrations for vandenbrandeite at a) 3614, b) 3576, c) 3555, d) 3445, e) 3408, f) 3400, g) 3365 and h) 3229 cm^{-1}. Blue represents U, brown as Cu, red O and white H.

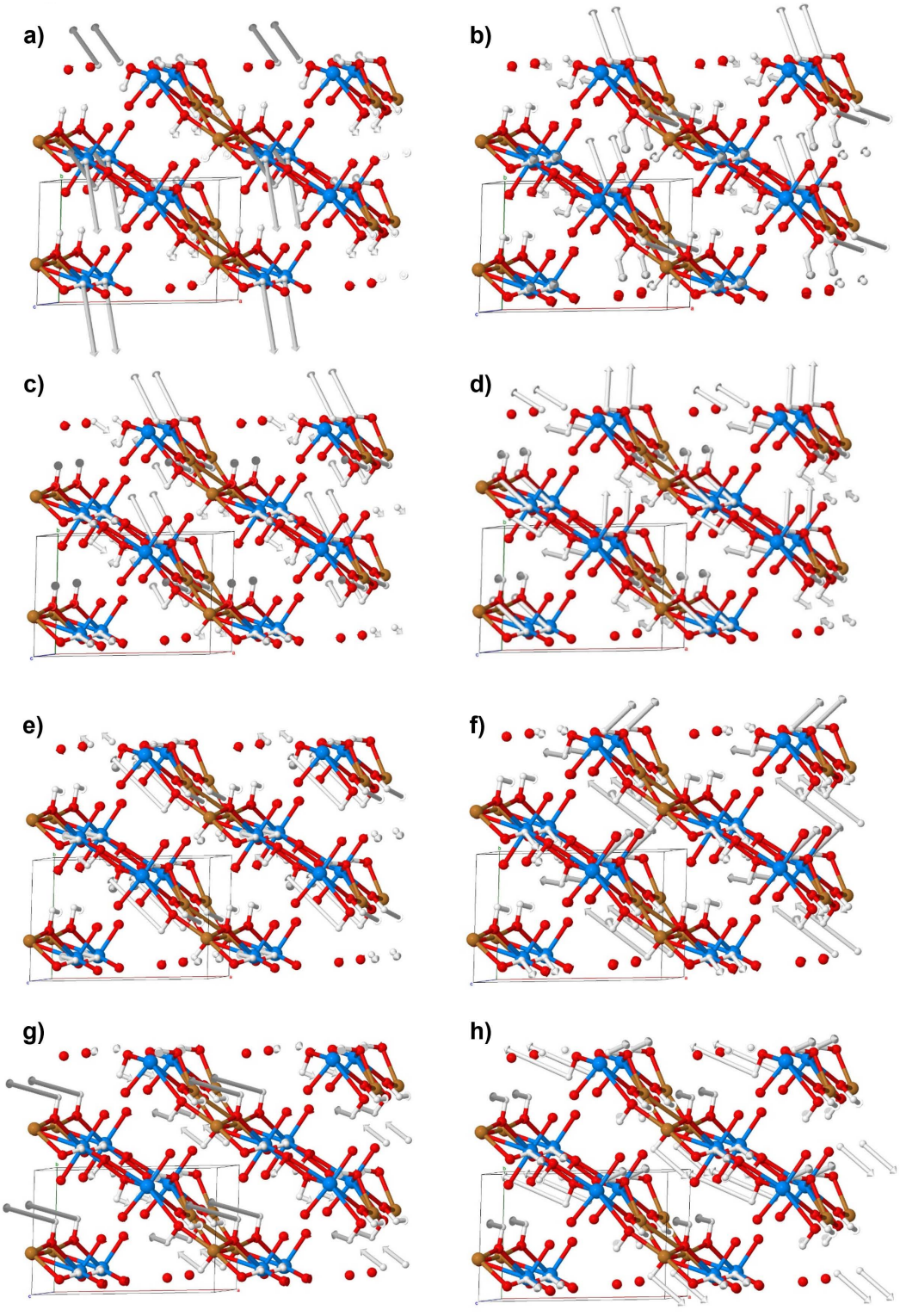

FIGURE S3: Raman vector bending motions of the free-hanging H bond connected to an equatorial uranyl O atom, δ(UOH), for vandenbrandeite at a) 1044, b) 1018, c) 1009, d) 974, e) 969, f) 947, g) 943 and h) 917 cm^{-1}. Blue represents U, brown as Cu, red O and white H.

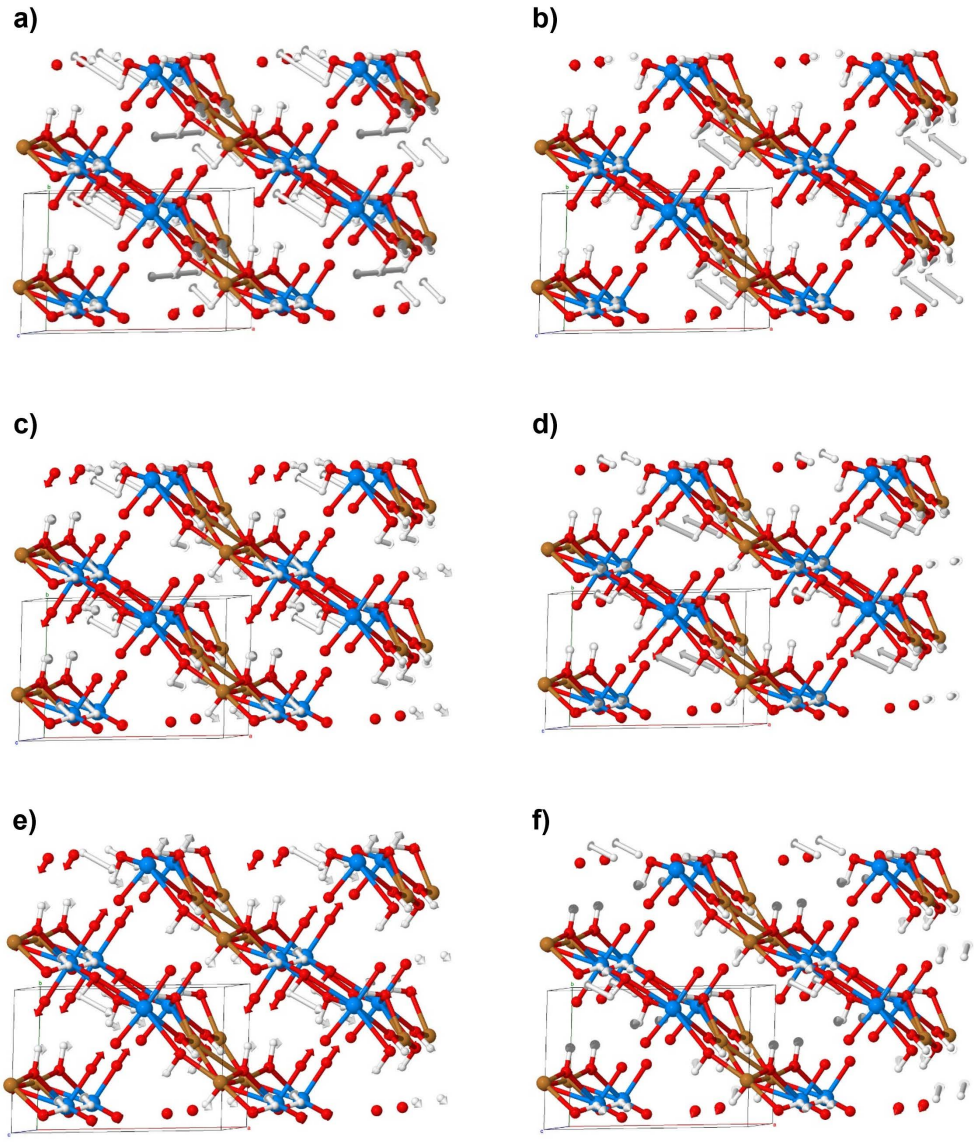

FIGURE S4: Raman vector images of the axial asymmetric uranyl stretching vibrations, $\nu_3(UO_2)^{2+}_{axial}$, at a) 889, b) 878 and c) 850 cm^{-1} and axial symmetric uranyl stretching vibrations, $\nu_1(UO_2)^{2+}_{axial}$, at d) 828, e) 800 and f) 791 cm^{-1}. All uranyl modes shown in this figure are accompanied by δ(UOH) vibrations. Blue represents U, brown as Cu, red O and white H.

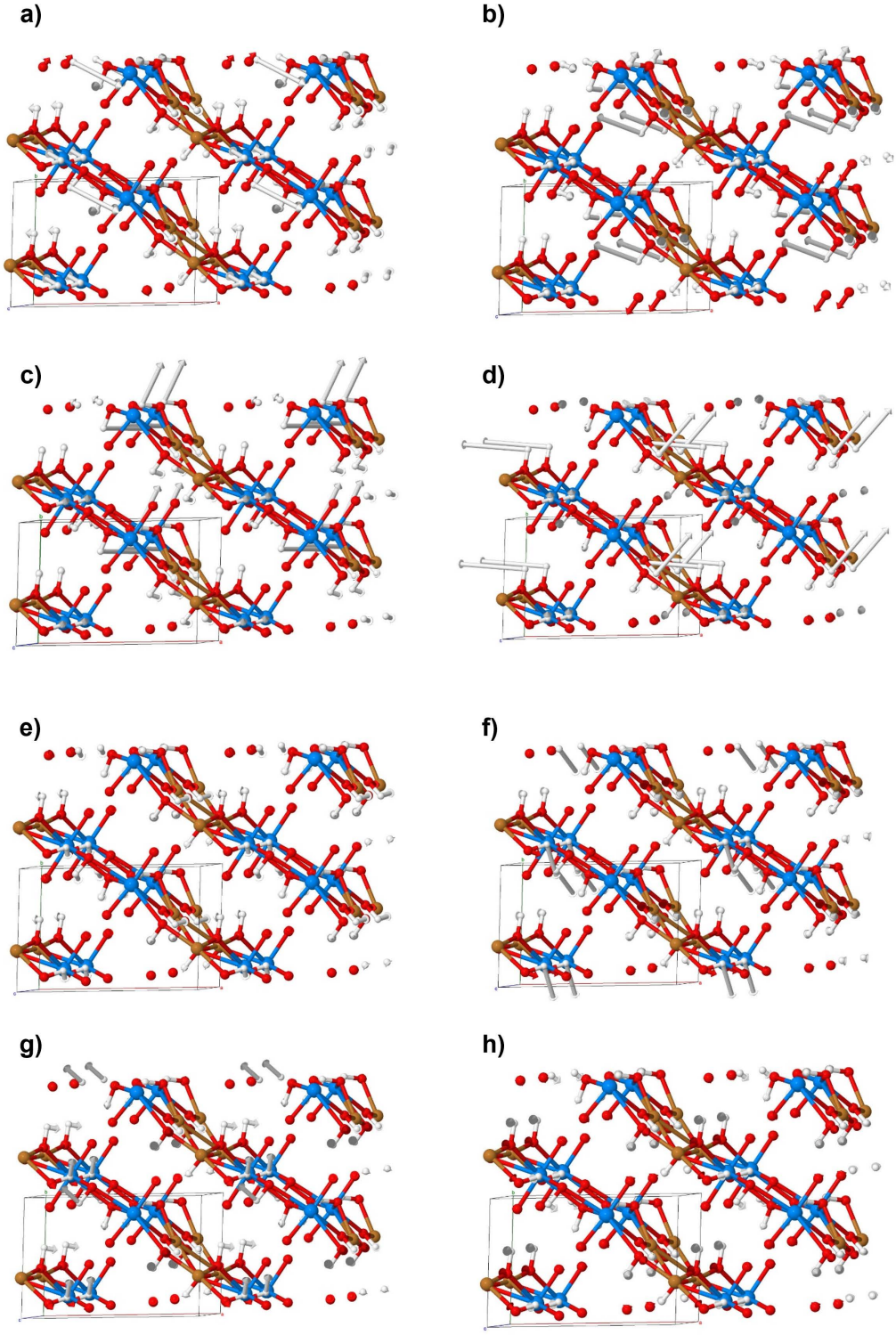

FIGURE S5: Simulated Raman vector vibration images for vandenbrandeite a) 780, b) 760, c) 734, d) 624, e) 579, f) 546, g) 496 and h) 493 cm^{-1}. Blue represents U, brown as Cu, red O and white H.

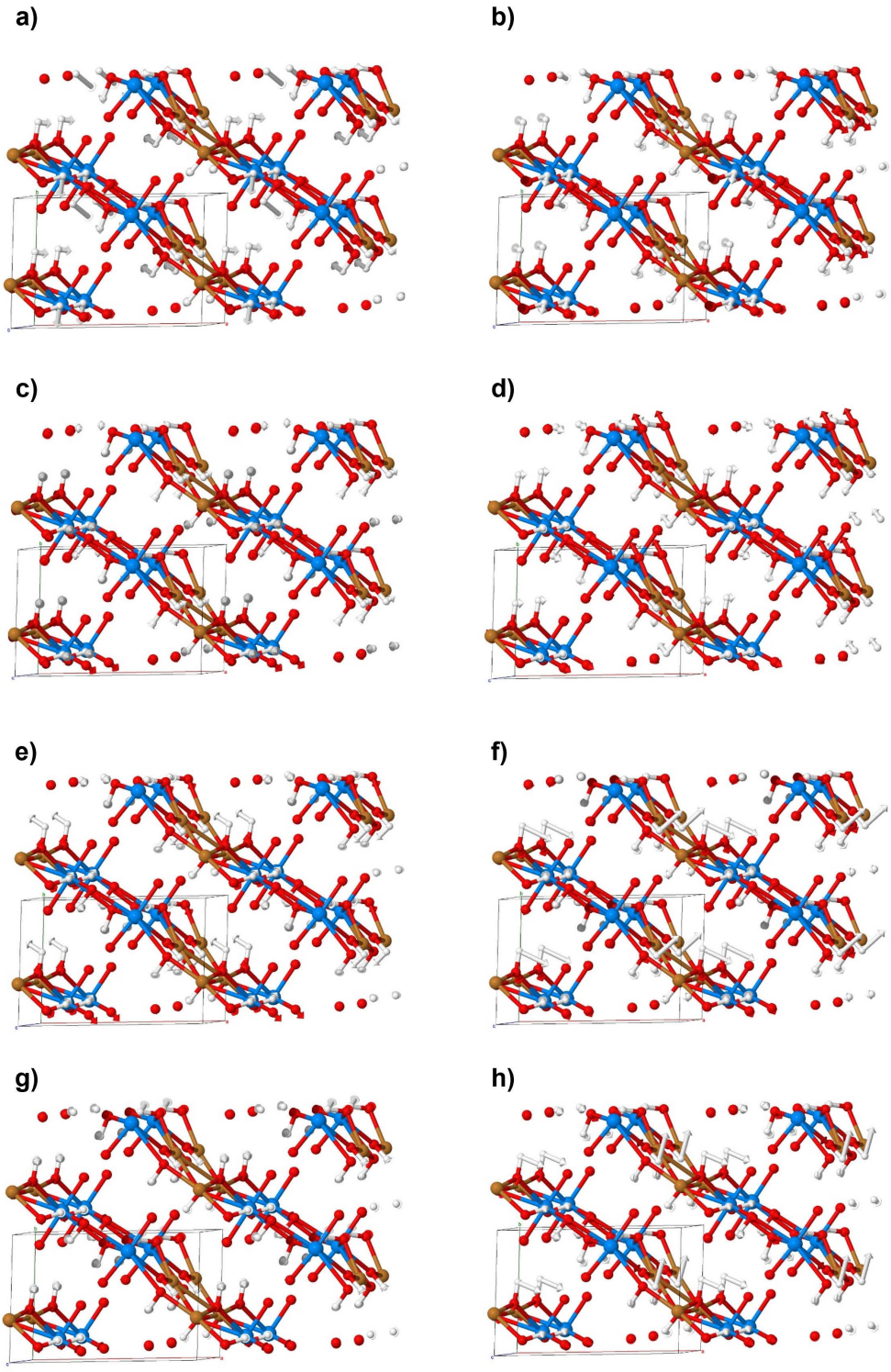

FIGURE S6: Simulated Raman vector vibration images for vandenbrandeite a) 484, b) 464, c) 446, d) 430, e) 403, f) 382, g) 372 and h) 366 cm^{-1}. Blue represents U, brown as Cu, red O and white H.

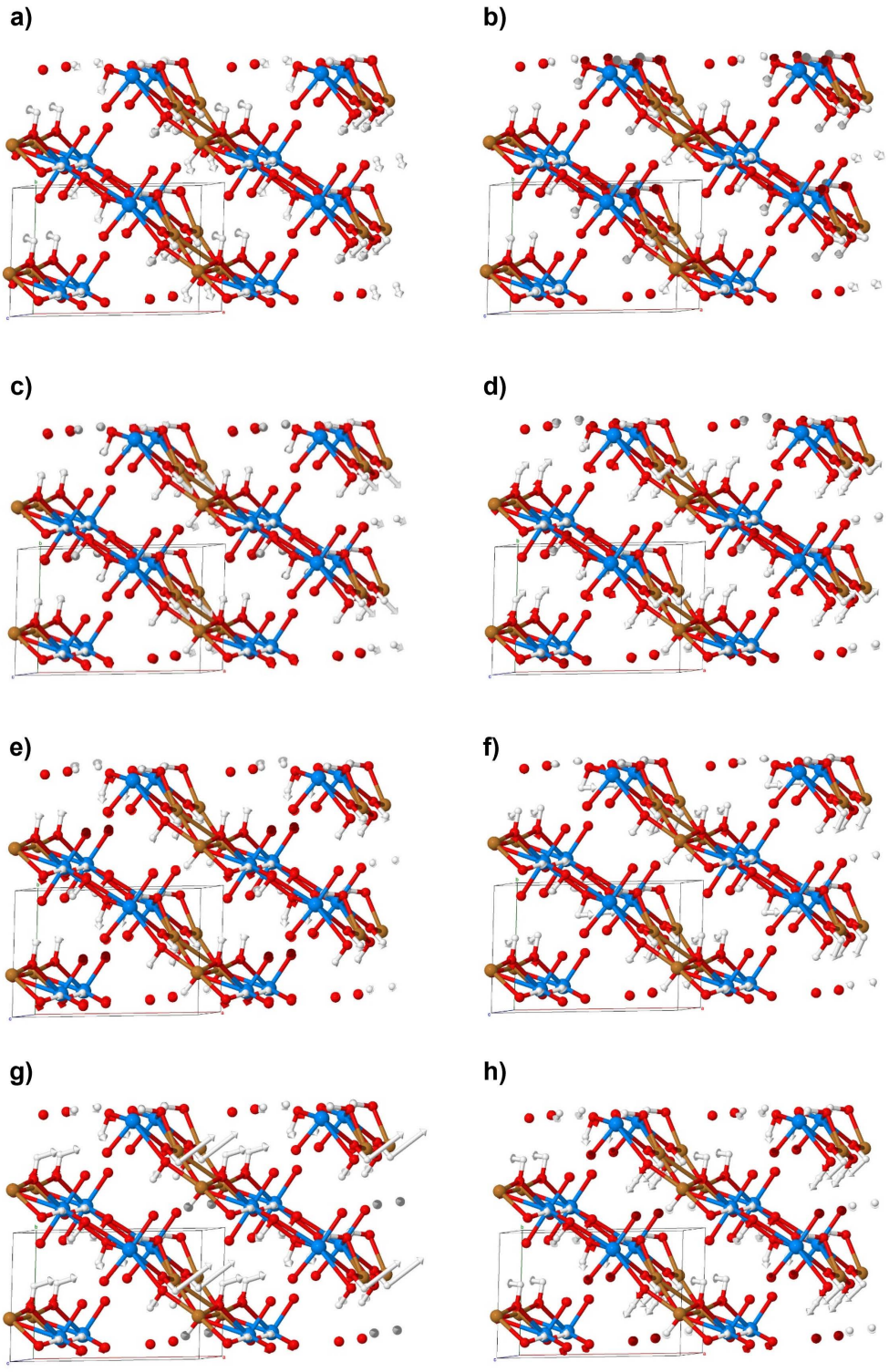

FIGURE S7: Simulated Raman vector vibration images for vandenbrandeite a) 350, b) 345, c) 320, d) 309, e) 293, f) 290, g) 277 and h) 268 cm^{-1}. Blue represents U, brown as Cu, red O and white H.

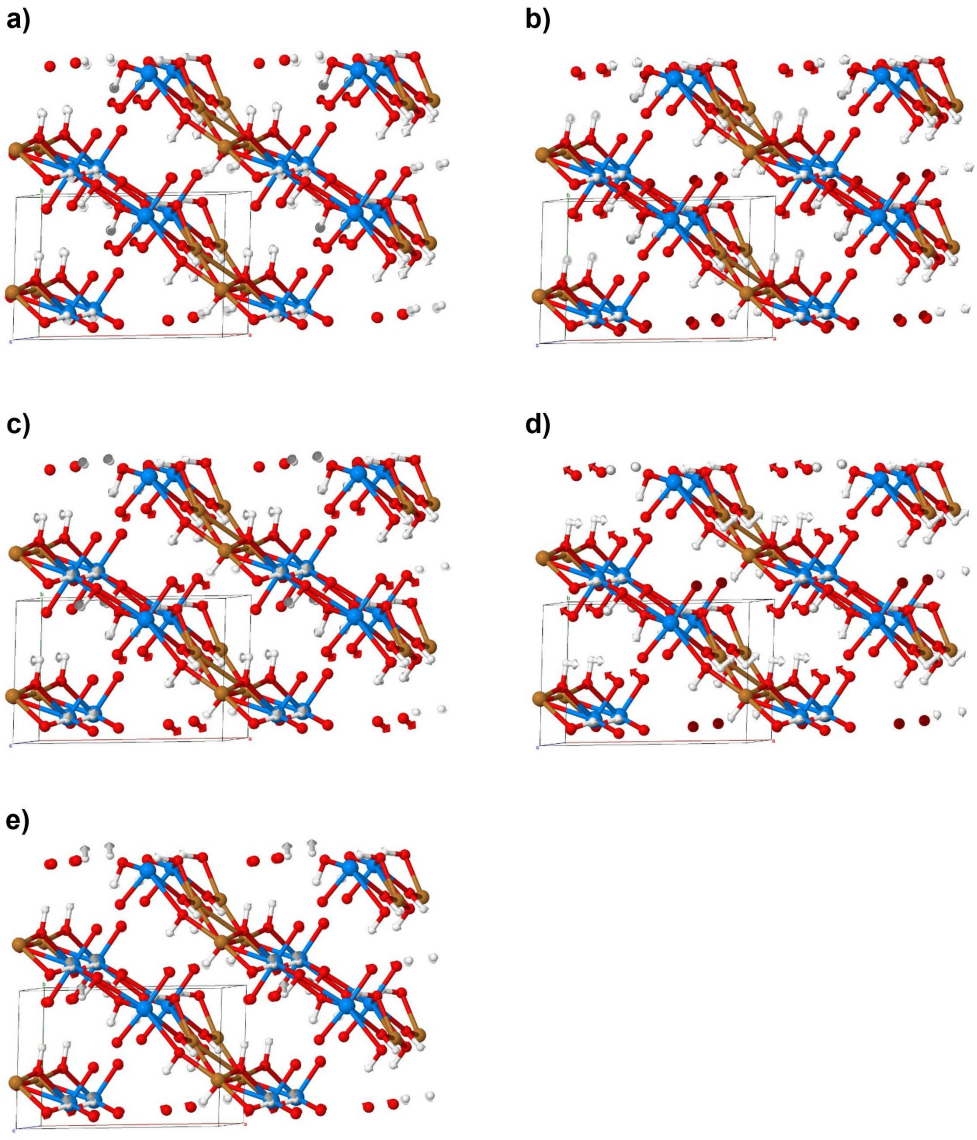

FIGURE S8: Axial uranyl symmetric bending, $v_2(UO_2)^{2+}_{axial}$, simulated Raman vector images for vandenbrandeite at a) 246, b) 244, c) 239, d) 230 and e) 222 cm^{-1}. Blue represents U, brown as Cu, red O and white H.

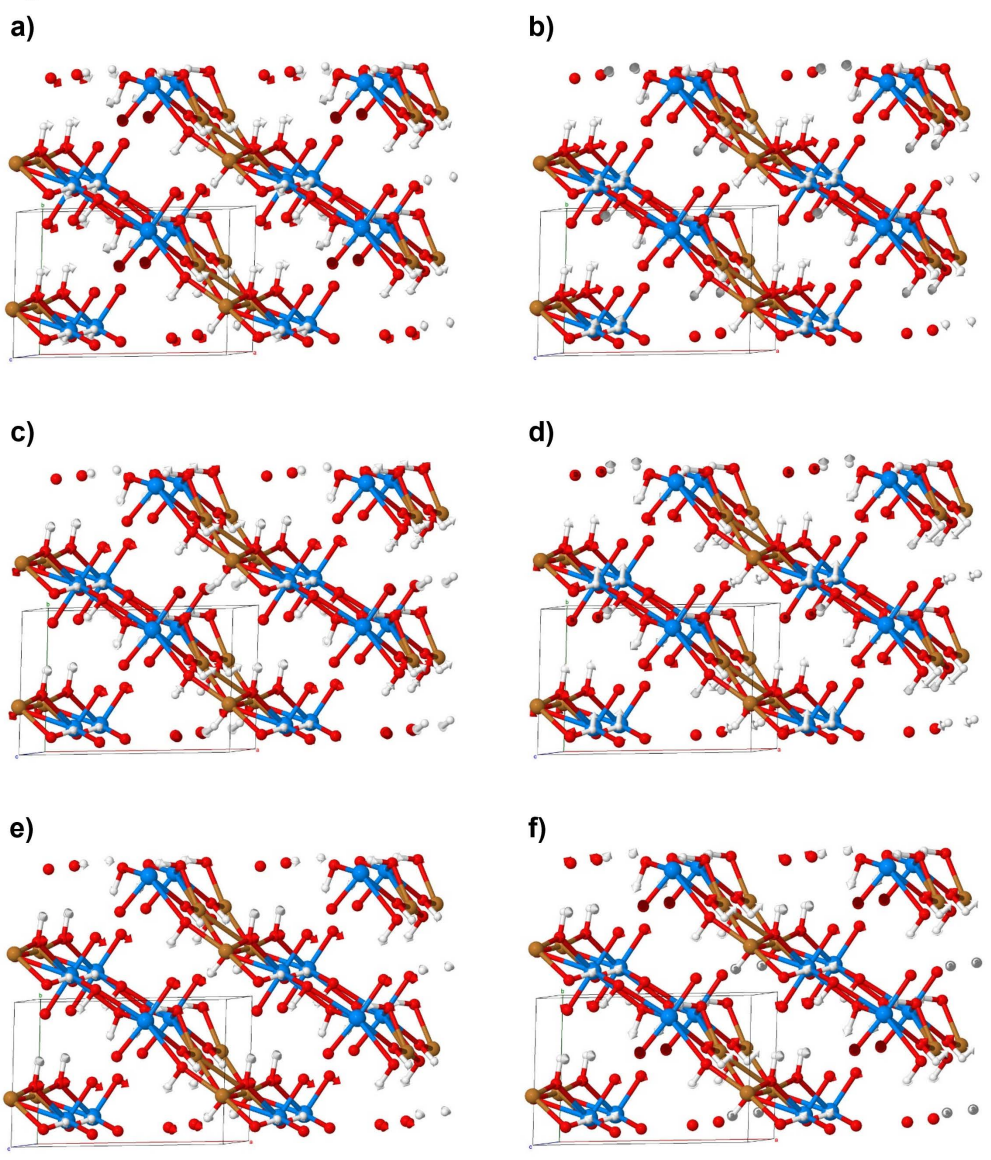

FIGURE S9: Simulated Raman lattice vibrations for vandenbrandeite at a) 215, b) 203, c) 196, d) 187, e) 175 and f) 162 cm^{-1}. Blue represents U, brown as Cu, red O and white H.

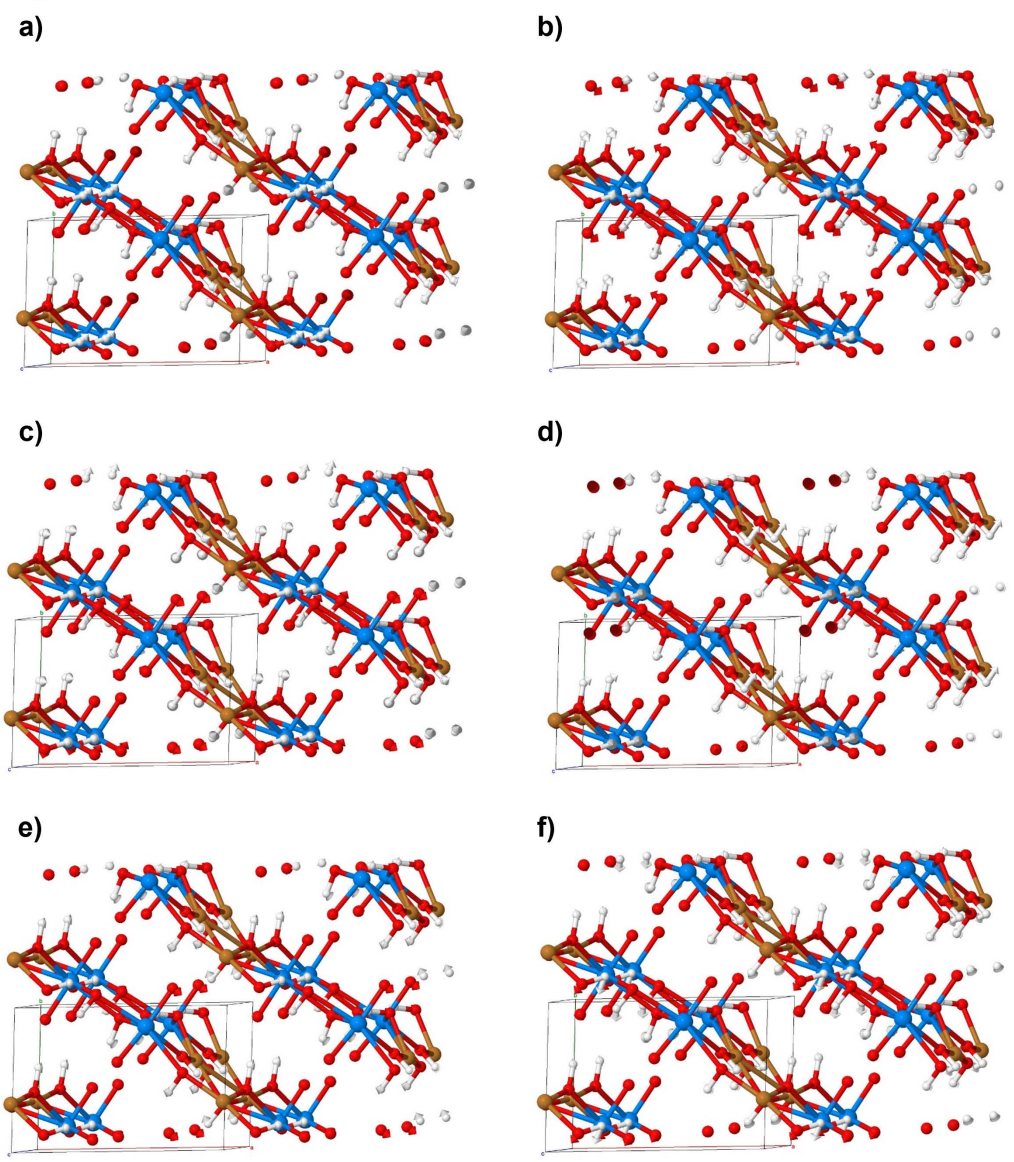

FIGURE S10: Simulated Raman lattice vibrations for vandenbrandeite at a) 156, b) 147, c) 132, d) 121, e) 114 and f) 109 cm^{-1}. Blue represents U, brown as Cu, red O and white H.

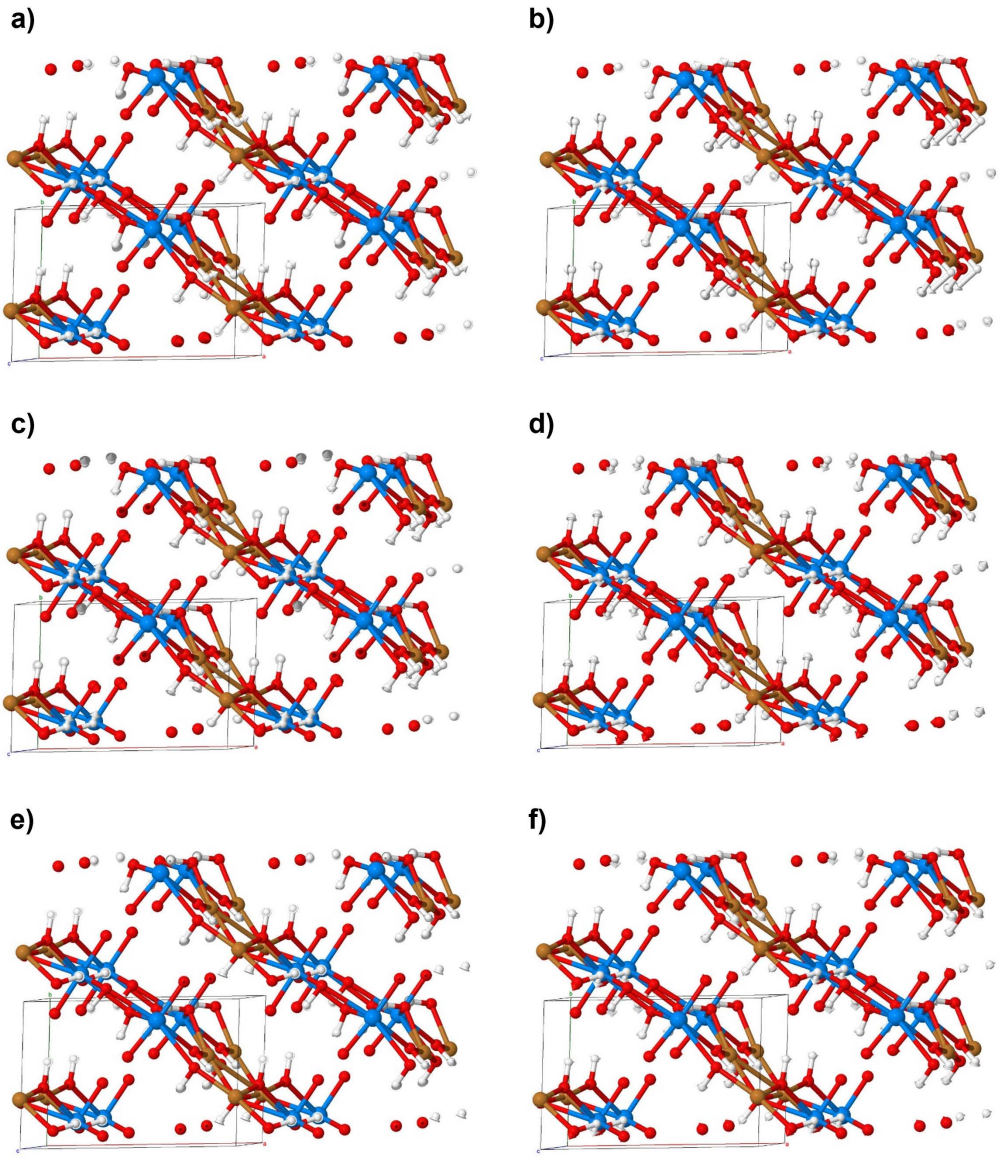

FIGURE S11: Simulated Raman lattice vibrations for vandenbrandeite at a) 99, b) 97, c) 78, d) 72, e) 57 and f) 43 cm^{-1}. Blue represents U, brown as Cu, red O and white H.